INTERNATIONAL JOURNAL FOR NUMERICAL METHODS IN FLUIDS, VOL. 8, 493–517 (1988)

A PETROV–GALERKIN METHOD FOR THE NUMERICAL SOLUTION OF THE BRADSHAW–FERRISS–ATWELL TURBULENCE MODEL

I. B. STEWART

University of Bristol Computer Centre, School of Mathematics, University Walk, Bristol BS8 1TW, U.K.

AND

K. UNSWORTH

Department of Mathematical Sciences, The University, Dundee DD1 4HN, U.K.

SUMMARY

The Bradshaw–Ferriss–Atwell model for 2D constant property turbulent boundary layers is shown to be ill-posed with respect to numerical solution. It is shown that a simple modification to the model equations results in a well-posed system which is hyperbolic in nature. For this modified system a numerical algorithm is constructed by discretizing in space using the Petrov–Galerkin technique (of which the standard Galerkin method is a special case) and stepping in the timelike direction with the trapezoidal (Crank–Nicolson) rule. The algorithm is applied to a selection of test problems. It is found that the solutions produced by the standard Galerkin method exhibit oscillations. It is further shown that these oscillations may be eliminated by employing the Petrov–Galerkin method with the free parameters set to simple functions of the eigenvalues of the modified system.

KEY WORDS Turbulent boundary layer flow Hyperbolic systems Finite element method Petrov–Galerkin method

1. INTRODUCTION

In this paper we shall use the finite element technique to construct an algorithm for numerically simulating one specific type of turbulent flow: the 2D turbulent wall boundary layer. The equations which govern 2D wall boundary layer flow are derived from the Navier–Stokes equations by either time or ensemble averaging techniques[1] and application of the boundary layer order of magnitude analysis.[2] The resulting equations—see equations (1) and (2)—are commonly known as the thin shear layer (TSL) equations and form a system of two equations in the three unknowns u and v, the mean velocities, and $-\rho\overline{u'v'}$, the Reynolds shear stress. To solve the TSL equations one must make certain hypotheses about the distribution of the Reynolds shear stress. This is called the closure problem and its solutions are known as 'closures' or 'turbulence models'. Details of and comparisons between a variety of turbulence models can be found in Launder and Spalding,[3] Haines,[4] Rodi[5,6] and Marvin.[7] One popular group of turbulence models is based on the eddy, or turbulent, viscosity concept in which an eddy, or turbulent, viscosity ν_t is defined by

$$-\overline{u'v'} = \nu_t \frac{\partial u}{\partial y}.$$

0271–2091/88/050493–25$12.50

Received 26 June 1986
Revised 8 May 1987

Dimensional arguments imply that the parameter ν_t is proportional to a characteristic velocity scale multiplied by a characteristic length scale. Prandtl proposed the form

$$\nu_t = l_m^2 \left| \frac{\partial u}{\partial y} \right|,$$

where l_m, the mixing length, is prescribed using empirical data. An example of a mixing length closure model is given by Cebeci and Smith.[2] More complex eddy viscosity models assume that $\sqrt{k}$, where k is the turbulent kinetic energy, is a characteristic velocity scale. Examples of this type are the k–L and k–ε closure models.[3,6] In the former a transport equation for k is constructed and the length scale L is specified algebraically. In the latter transport equations for k and the dissipation ε are constructed and the length scale L is related to the dissipation by the relation

$$\varepsilon = C_D k^{3/2}/L,$$

where C_D is a constant.

The model employed in this paper is the Bradshaw, Ferriss and Atwell (henceforth denoted BFA) turbulence model[8] which differs from those described above in that it does not employ the eddy viscosity concept. Instead, since experimental evidence suggested that $k \propto \overline{u'v'}$, the turbulent kinetic energy equation is converted into a transport equation for the Reynolds shear stress. Therefore the BFA model is really the simplest of the family of shear stress transport models of which brief descriptions can be found in Marvin.[7]

The basic numerical techniques required for solving problems in fluid mechanics are well documented in the texts by Roache[9] for finite differences and by Baker[10] and Connor and Brebbia[11] for the finite element method. The paper by Hutton[12] reviews suitable finite element techniques for general viscous incompressible flow problems. Comprehensive theoretical treatments of the finite element method are given by Strang and Fix[13] and Mitchell and Wait.[14] Petrov–Galerkin, or generalized Galerkin, methods have been developed and applied by Christie *et al.*,[15,16] Mitchell and Griffiths[17,18] and Morton and Parrott.[19] For the mixing length and k–ε turbulence models finite element algorithms have been proposed by Baker,[10] Hutton,[12] Hutton and Smith,[20] Launder and Spalding,[21] Morgan *et al.*,[22,23] Soliman *et al.*,[24] Smith[25,26] and Taylor *et al.*[27]

Section 2 gives a brief outline of the BFA turbulence model. The mathematical properties of the system of equations are investigated in Section 3. The system will be shown to be of hyperbolic type, and the equations of the characteristic curves and the equations of the ordinary differential equations along those curves will be derived. The numerical solution method will be constructed in Section 4 and a selection of the numerical results obtained is given in Section 5.

2. THE TURBULENCE MODEL

The turbulence model as described in this paper is only applicable to one class of external flow, i.e., steady, two-dimensional, constant property (i.e., constant viscosity and constant density), turbulent boundary layer flow over a smooth flat plate.

The flow external to the boundary layer is assumed to be in steady irrotational motion and the flow within the boundary layer is assumed to be fully turbulent. The mean flow is assumed to be two-dimensional in the x–y plane with the external flow moving parallel to the x axis. The two components of the mean velocity vector are u, the longitudinal velocity, and v, the transverse velocity. The fixed boundary, or wall, is positioned at $y = 0$.

At the fixed boundary the no-slip condition holds and at the outer edge of the boundary layer the velocity u tends asymptotically to the free stream velocity u_e. We assume that there is no suction or

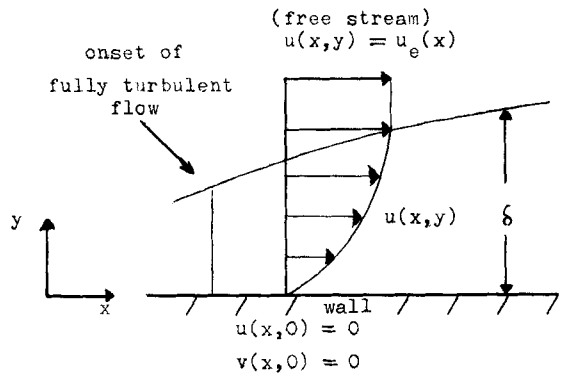

Figure 1. Geometry of the turbulent boundary layer problem

injection of fluid at the wall boundary. Therefore we have the physical boundary conditions

$$u(x, y=0)=0, \qquad u(x, y\to\infty)=u_e, \qquad v(x, y=0)=0.$$

The boundary layer thickness δ is conventionally defined to be the distance along the y axis at which $u = 0{\cdot}995\, u_e$. For numerical calculation the outer edge boundary condition is usually applied at a distance $y=\delta_+$, where δ_+ is a finite distance larger than δ. The geometry of the problem is illustrated in Figure 1.

The mean motion of the fluid for boundary layers is modelled by the well-known thin shear layer (TSL) equations[1,2]

$$\rho\left(u\frac{\partial u}{\partial x}+v\frac{\partial u}{\partial y}\right)=\rho u_e\frac{du_e}{dx}+\frac{\partial}{\partial y}\left(\mu\frac{\partial u}{\partial y}-\rho\overline{u'v'}\right), \tag{1}$$

$$\rho\left(\frac{\partial u}{\partial x}+\frac{\partial v}{\partial y}\right)=0, \tag{2}$$

where $\nu=\mu/\rho$, u and v are the components of the mean velocity vector and u' and v' are two of the components of the fluctuating velocity vector. Equation (1) is the mean momentum equation and equation (2) is the mean conservation of mass (continuity) equation. As we have assumed that the flow has constant density, we shall henceforth assume, without loss of generality, that ρ is a constant equal to 1.

The term in parentheses on the right-hand side of (1),

$$\mu\frac{\partial u}{\partial y}-\rho\overline{u'v'}, \tag{3}$$

is the total shear stress, commonly denoted τ, and is the sum of the viscous (left-hand term) and turbulent (right-hand term) stresses. For turbulent boundary layer flows it can be shown that the viscous stress term in (3) is the dominant term only in a very thin layer close to the wall.[1] Outside of this layer it has small magnitude compared with the Reynolds stress and thus may be neglected. The TSL equations for 2D constant property turbulent boundary layer flow are therefore a system of two equations in the three unknowns u, v and $-\rho\overline{u'v'}$.

The BFA closure model consists of an empirical transport equation for the Reynolds shear stress derived from the turbulent kinetic energy equation which, for 2D constant property flow without body forces, is[1]

$$u\frac{\partial}{\partial x}(k)+v\frac{\partial}{\partial y}(k)=-\overline{u'v'}\,\frac{\partial u}{\partial y}-\frac{\partial}{\partial y}\left(\frac{1}{\rho}\overline{p'v'}+\overline{kv'}\right)-\varepsilon, \tag{4}$$

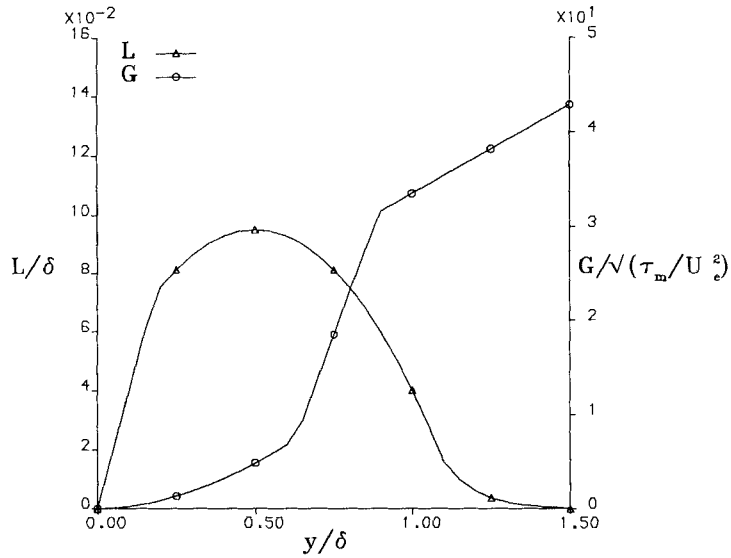

Figure 2. The empirical functions L and G

where all the viscous terms except the dissipation have been treated as negligible.

To derive the model, the following closure quantities are defined:

$$a_1 := \tau/2k, \tag{5}$$

$$L := \tau^{3/2}/\varepsilon, \tag{6}$$

$$G := (\overline{p'v'} + \overline{kv'})/\tau\tau_m^{1/2}, \tag{7}$$

where a_1 is the ratio of the shear stress to twice the turbulent kinetic energy, L is a dissipation length scale and G is a diffusion function. a_1 and G are dimensionless, while L has the dimensions of length. The parameter τ_m is chosen to be the maximum shear stress in the region $[\delta/4, \delta]$. Bradshaw *et al.*[8] give full details concerning the definition, justification and measurement of the above quantities. The values chosen by Bradshaw *et al.* for these functions are

$$a_1 = 0{\cdot}15, \qquad L/\delta = f(y/\delta), \qquad G = \sqrt{(\tau_m/U_e^2)}\, g(y/\delta).$$

Figure 2 illustrates L and G. Townsend[28] gives justification for the particular value chosen for a_1.

Substituting expressions (5)–(7) into equation (4) results in the following empirical transport equation for the Reynolds shear stress:

$$u\frac{\partial}{\partial x}\left(\frac{\tau}{2a_1}\right) + v\frac{\partial}{\partial y}\left(\frac{\tau}{2a_1}\right) = \tau\frac{\partial u}{\partial y} - \frac{\partial}{\partial y}(G\tau\tau_m^{1/2}) - \frac{\tau^{3/2}}{L}. \tag{8}$$

Notes

(1) The specification of a_1 as a constant restricts the model to flows where the Reynolds stress does not change sign, such as boundary layers. However, there have been modifications which allow the treatment of duct flows, jets and wakes.[6]

(2) For the BFA turbulence model given above, the length scale L is specified by an algebraic relation. A length scale transport equation has been developed by Bradshaw.[29]

3. MATHEMATICAL PROPERTIES OF THE TURBULENCE MODEL EQUATIONS

The natural notation for quasilinear first-order systems is the matrix form

$$\mathbf{A}(\mathbf{w}, x, y)\mathbf{w}_x + \mathbf{B}(\mathbf{w}, x, y)\mathbf{w}_y = \mathbf{C}(\mathbf{w}, x, y). \tag{9}$$

For the BFA system of equations $\mathbf{A}$ and $\mathbf{B}$ are the 3×3 matrices

$$\mathbf{A} = \begin{bmatrix} u & 0 & 0 \\ 1 & 0 & 0 \\ 0 & 0 & u \end{bmatrix}, \quad \mathbf{B} = \begin{bmatrix} v & 0 & -1 \\ 0 & 1 & 0 \\ -2a_1\tau & 0 & v + 2a_1\tau_m^{1/2} G \end{bmatrix} \tag{10a}$$

and $\mathbf{w}$ and $\mathbf{C}$ are the 3-vectors

$$\mathbf{w} = (u, v, \tau)^T, \qquad \mathbf{C} = \left(u_e \frac{du_e}{dx}, 0, -2a_1 \left(\tau_m^{1/2} \frac{dG}{dy} \tau + \frac{\tau^{3/2}}{L} \right) \right)^T, \tag{10b}$$

where $(x, y) \in [x_0, X] \otimes [\xi, \delta_+]$, the point $y = \xi$ lies in the logarithmic law region, i.e., $u_\tau y/\nu > 30$–50, and $\delta_+ > \delta$. Associated with (9), (10) are the initial conditions, at $x_0 = 0$ say,

$$u(0, y) = u_0(y), \qquad v(0, y) = v_0(y), \qquad \tau(0, y) = \tau_0(y). \tag{11a}$$

As viscous effects near the wall have been neglected, the model is valid only outside the viscous sublayer close to the wall and so bridging functions, such as the logarithmic law,[1,30] must be used to impose the numerical near-wall boundary conditions at $y = \xi$. Therefore the boundary conditions associated with (9), (10) are of the form

$$u(x, \xi) = u_\tau \left[\frac{1}{\kappa} \ln \left(\frac{u_\tau \xi}{\nu} \right) + C \right], \qquad u(x, \delta_+) = u_e(x), \qquad v(x, \xi) = -\xi u(x, \xi) \frac{d}{dx}(\ln u_\tau), \tag{11b}$$

where κ and C are constants.

The set of equations (9)–(11) describes an initial boundary value problem (IBVP) for a quasilinear first-order system in which the independent variables x and y are such that x is treated as a timelike variable and y as the spatial variable.

For a general 3×3 system of quasilinear first-order equations we can define hyperbolicity as follows.

Definition[31]

The general first-order quasilinear system (9) is said to be hyperbolic in the x direction at a point P if the zeros λ_i, $i = 1, 2, 3$, of the characteristic polynomial

$$Q(P, \lambda) := \det(\mathbf{A}(P)\lambda - \mathbf{B}(P))$$

are all real and if the left eigenvectors $\mathbf{l}_i$, $i = 1, 2, 3$, satisfying

$$\mathbf{l}_i^T(\mathbf{A}(P)\lambda_i - \mathbf{B}(P)) = 0, \quad i = 1, 2, 3, \tag{12}$$

form a set of three linearly independent vectors in $\mathbb{R}^3$.

Assuming that system (9) is hyperbolic, we can determine the set of characteristic curves $\mathscr{C}_i$, $1, 2, 3$, in x–y space by solving

$$\mathscr{C}_i : \frac{dy}{dx} = \lambda_i(\mathbf{w}, x, y), \qquad i = 1, 2, 3. \tag{13}$$

Equivalently, by introducing a parameter s, we can assign a direction vector $(1, \lambda_i)$ to points $x(s)$, $y(s)$ where

$$\frac{dy}{ds} = \lambda_i(\mathbf{w}, x, y), \qquad \frac{dx}{ds} = 1, \qquad i = 1, 2, 3. \tag{14}$$

Using (12), we may write (9) in the characteristic normal form

$$\mathbf{LAw}_x + \mathbf{\Lambda LAw}_y = \mathbf{LC} \tag{15}$$

where the rows of $\mathbf{L}$ are the independent left eigenvectors and $\mathbf{\Lambda} = \text{diag}(\lambda_1, \lambda_2, \lambda_3)$. In component form (15) is

$$\sum_{j=1}^{3} a_{ij}\left(\frac{\partial}{\partial x} + \lambda_i \frac{\partial}{\partial y}\right) w_j = c_i, \qquad i = 1, 2, 3, \tag{16}$$

where

$$a_{ij} = L_{ik}A_{kj}, \qquad c_i = L_{ik}C_k.$$

Using (13) and (14), the system of partial differential equations given by (16) can be written as the system of ordinary differential equations

$$\sum_{j=1}^{3} a_{ij}\frac{dw_j}{ds} = \frac{dx}{ds}c_i, \qquad i = 1, 2, 3, \tag{17}$$

where s characterizes the curve $\mathscr{C}_i$ and is defined by

$$\frac{dy}{ds} = \lambda_i(\mathbf{w}, x(s), y(s))\frac{dx}{ds}, \qquad i = 1, 2, 3. \tag{18}$$

The two sets of equations (17) and (18) comprise the set of equations solved by the method of characteristics.

We now examine the Cauchy problem for the general first-order quasilinear system (9), i.e., the pure initial value problem consisting of (9) together with prescribed data on the initial curve.

The Cauchy–Kowalesky theorem[32] states that if the initial data are specified on a non-characteristic line, a unique solution to the Cauchy problem exists in a neighbourhood of the initial line. However, if the initial line is characteristic, which occurs whenever $\det(\mathbf{A}) = 0$, then the solution does not exist unless certain constraints are satisfied, and even if it does exist the solution is in general non-unique.

Richtmyer[33] shows that when an initial line is characteristic, a necessary condition for the existence of a solution to the Cauchy problem is that the initial data $\mathbf{w}(x = x_0, y)$ satisfies the differential relationship

$$\mathbf{l}^{\mathrm{T}}(0)\mathbf{Bw}_y = \mathbf{l}^{\mathrm{T}}(0)\mathbf{C}, \tag{19}$$

where $\mathbf{l}^{\mathrm{T}}(0)$ is the left eigenvector of $\mathbf{A}$ corresponding to the zero eigenvalue of $\mathbf{A}$.

For the particular system defined by (9)–(11) it is easily seen that $\det(\mathbf{A}) = 0$. Thus there exists a family of characteristic curves with equation $x = \text{constant}$; in particular the initial line is characteristic. Therefore the problem as stated is not well-posed. From (19), in order for a solution to (9)–(11) to exist, the following ordinary differential equation must be satisfied:

$$v\frac{du}{dy} - u\frac{dv}{dy} - \frac{d\tau}{dy} = u_e\frac{du_e}{dx}. \tag{20}$$

Furthermore, as written, the system (9)–(11) is ill-posed with respect to any numerical solution

method which employs a time (x direction) marching scheme. For example, stability requirements for explicit time marching schemes imply a zero-length time step. Using implicit marching schemes results in oscillatory values for the v component. To overcome this ill-posedness of the problem, we reformulate (9)–(11) as the 2×2 system

$$\mathbf{A}(\mathbf{w}, x, y)\mathbf{w}_x + \mathbf{B}(\mathbf{w}, x, y)\mathbf{w}_y = \mathbf{C}(\mathbf{w}, x, y), \tag{21a}$$

where

$$\mathbf{A} = \begin{bmatrix} u & 0 \\ 0 & u \end{bmatrix}, \qquad \mathbf{B} = \begin{bmatrix} v & -1 \\ p^2 - q^2 & v + 2p \end{bmatrix}, \tag{21b}$$

$$\mathbf{w} = (u, \tau)^{\mathrm{T}}, \qquad \mathbf{C} = \left(u_{\mathrm{e}} \frac{\mathrm{d}u_{\mathrm{e}}}{\mathrm{d}x}, -2a_1 \left(\tau_{\mathrm{m}}^{1/2} \frac{\mathrm{d}G}{\mathrm{d}y} \tau + \frac{\tau^{3/2}}{L} \right) \right)^{\mathrm{T}}, \tag{21c}$$

$$p = a_1 G \tau_{\mathrm{m}}^{1/2}, \qquad q = (p^2 + 2a_1 \tau)^{1/2}$$

and the velocity v is assumed known or calculable.

Proceeding with the method of analysis outlined previously, we find that (21) is hyperbolic in the x direction with eigenvalues given by

$$\lambda_1 = \frac{v + p + q}{u}, \qquad \lambda_2 = \frac{v + p - q}{u}, \tag{22}$$

and corresponding left eigenvectors

$$\mathbf{l}_1 = \begin{bmatrix} p - q \\ 1 \end{bmatrix}, \qquad \mathbf{l}_2 = \begin{bmatrix} p + q \\ 1 \end{bmatrix}.$$

The two families of characteristic curves are defined by

$$\mathscr{C}_{1,2}: \frac{\mathrm{d}y}{\mathrm{d}s} = \left(\frac{v + p \pm q}{u} \right) \frac{\mathrm{d}x}{\mathrm{d}s} \tag{23}$$

and the characteristic normal form of the system is

$$\frac{\mathrm{d}u}{\mathrm{d}s} - \frac{p \pm q}{2a_1 \tau} \frac{\mathrm{d}\tau}{\mathrm{d}s} = \frac{1}{u} \left[u_{\mathrm{e}} \frac{\mathrm{d}u_{\mathrm{e}}}{\mathrm{d}x} + (p \pm q) \left(\frac{\mathrm{d}G}{\mathrm{d}y} \tau_{\mathrm{m}}^{1/2} + \frac{\tau^{1/2}}{L} \right) \right] \frac{\mathrm{d}x}{\mathrm{d}s}. \tag{24}$$

Using the property that the angles between the characteristic curves and the x axis are given by

$$\tan \eta_i = \lambda_i,$$

we can state the following:

(1) Near the wall, but outside the viscous sublayer, $G \ll \tau$ and the curves are at approximately equal and opposite angles to the x axis,

(2) Near the boundary layer edge $\tau \ll G$ and so one characteristic curve coincides with the streamline while the other nominally coincides with the boundary layer edge.[8]

The hyperbolicity of (21) leads to the Courant–Friedrichs–Lewy (CFL) stability criterion which restricts the time step for explicit marching schemes. This condition requires

$$x_{\mathrm{step}} = \Delta x = \frac{\Delta y}{\max\limits_{\xi \leq y \leq \delta_+} \{|\lambda_1|, |\lambda_2|\}}, \tag{25}$$

where Δy is some discretization interval in the y direction.

Initial and boundary conditions

For the system (21) the correct initial data to prescribe, on $x_0 = 0$ say, for a well-posed problem are the Cauchy data

$$u_1(0, y) = u_0(y), \qquad \tau_1(0, y) = \tau_0(y), \qquad \xi \leqslant y \leqslant \delta_+. \tag{26}$$

The number of boundary conditions that must be imposed at a point on the boundary is governed by the characteristic curves at that point. One is allowed to impose as many boundary conditions as there are characteristics entering into the solution domain from the boundary. If as is the case with (21) a characteristic is coincident with a boundary, the number of conditions is equal to the number of entrant characteristic curves excluding the boundary characteristic. Therefore one condition at each boundary can be imposed and we choose

$$u_B(x, \xi) = u_\tau \left[\frac{1}{\kappa} \ln\left(\frac{u_\tau \xi}{\nu} \right) + C \right], \qquad u_B(x, \delta_+) = u_e(x). \tag{27}$$

Imposing consistency conditions at $(0, \xi)$ and $(0, \delta_+)$, i.e.,

$$u_1(0, \xi) = u_B(0, \xi), \qquad u_1(0, \delta_+) = u_B(0, \delta_+), \tag{28}$$

we can state, using existence and uniqueness theorems,[32] that the IBVP given by (21), (26) and (27), where (26) and (27) satisfy (28), has a unique solution in some neighbourhood of $x > 0$, $\xi \leqslant y \leqslant \delta_+$. Note that the use of the logarithmic law to specify the near-wall boundary condition has introduced an additional unknown parameter $\tau_w^{1/2}(x) = u_\tau$.

4. THE SOLUTION METHOD

The solution method entails discretizing system (21) in the spatial direction using the Petrov–Galerkin technique and marching the resulting system of non-linear ordinary differential equations in time (x direction) using the θ method.

Considering Ω to be an interval $[\xi, \delta_+]$ of $\mathbb{R}$, we define a partition Δ on Ω as

$$\Delta: \xi = y_1 < y_2 < \cdots < y_{N+1} = \delta_+,$$

with an associated uniform step length $h = y_{j+1} - y_j$, $1 \leqslant j \leqslant N$.

Stating the problem as

$$\mathbf{A}(\mathbf{w})\mathbf{w}_x + \mathbf{B}(\mathbf{w})\mathbf{w}_y = \mathbf{C}(\mathbf{w}), \tag{29a}$$

with initial and boundary conditions

$$\mathbf{w}(0, y) = \mathbf{w}_0(y), \tag{29b}$$

$$w_1(x, \xi) = b_1, \qquad w_1(x, \delta_+) = b_2, \tag{29c}$$

where **A**, **B** and **C** are defined by (21b, c) and $\mathbf{w} = (w_1, w_2)^T = (u, \tau)^T$, we define the weak formulation of (29) to be:[14,17]

Find $\mathbf{w} = (u, \tau)^T$, where $u \in H_b^1(\Omega)$, $\tau \in H^1(\Omega)$, such that

$$(\mathbf{A}(\mathbf{w})\mathbf{w}_x + \mathbf{B}(\mathbf{w})\mathbf{w}_y - \mathbf{C}(\mathbf{w}), \mathbf{z}) = 0,$$

$$(\mathbf{w}(0, y) - \mathbf{w}_0(y), \mathbf{z}) = 0,$$

for all $\mathbf{z} = (z_1, z_2)^T$, where $z_1 \in H_0^1(\Omega)$, $z_2 \in H^1(\Omega)$ and the inner product is defined as

$$(\mathbf{w}, \mathbf{z}) = \int_\Omega \mathbf{w}^T \mathbf{z} \, dy, \qquad \mathbf{w}, \mathbf{z} \in L_2(\Omega).$$

The Galerkin approximation $\mathbf{W} = (U(x, y), T(x, y))^{\mathrm{T}}$ to $\mathbf{w} = (u, \tau)^{\mathrm{T}}$ is defined to be

$$\mathbf{W}(x, y) = \sum_{i=1}^{N+1} W_i(x)\varphi_i(y) = \sum_{i=1}^{N+1} \begin{pmatrix} U_i(x) \\ T_i(x) \end{pmatrix} \varphi_i(y). \tag{30}$$

Choosing the trial functions to be the usual linear 'hat' functions, defined away from the boundaries by

$$\varphi_j(y) = \left\{ \begin{array}{ll} 1+s, & -1 \leqslant s \leqslant 0 \\ 1-s, & 0 \leqslant s \leqslant 1 \\ 0 & |s| > 1 \end{array} \right\}, \qquad s = y/h - j, \tag{31}$$

application of the boundary conditions to (30) yields

$$W_1(x, y_1) = b_1, \qquad W_1(x, y_{N+1}) = b_2$$

and we therefore have a set of $2N$ unknowns

$$U_j(x), \qquad j = 2, \ldots, N; \qquad T_j(x), \qquad j = 1, \ldots, N+1.$$

Choosing test functions to be

$$\psi_k(y) = \begin{pmatrix} 1 \\ 0 \end{pmatrix} (\varphi_j(y) + \gamma^1 \sigma_j(y)), \qquad j = 2, \ldots, N; \qquad k = j - 1,$$

$$\psi_k(y) = \begin{pmatrix} 0 \\ 1 \end{pmatrix} (\varphi_j(y) + \gamma^2 \sigma_j(y)), \qquad j = 1, \ldots, N+1; \qquad k = N - 1 + j, \tag{32}$$

where γ^1 and γ^2 are free parameters and σ_j is a quadratic perturbation function[17,18,34] defined away from the boundaries by

$$\sigma_j(y) = \left\{ \begin{array}{ll} -3s(1+s), & -1 \leqslant s \leqslant 0 \\ -3s(1-s), & 0 \leqslant s \leqslant 1 \\ 0, & |s| > 1 \end{array} \right\}, \qquad s = y/h - j,$$

we can state the semi-discrete Petrov–Galerkin method for (29) as:

Find

$$\mathbf{W}(x, y) = \sum_{i=1}^{N+1} \begin{pmatrix} U_i(x) \\ T_i(x) \end{pmatrix} \varphi_i(y) \tag{33a}$$

such that

$$(\mathbf{A}(\mathbf{W})\mathbf{W}_x + \mathbf{B}(\mathbf{W})\mathbf{W}_y - \mathbf{C}(\mathbf{W}), \psi_k) = 0, \qquad k = 1, \ldots, 2N, \tag{33b}$$

and

$$(\mathbf{W}(0, y) - \mathbf{w}_0(y), \psi_k) = 0, \tag{33c}$$

where

$$W_1(x, y_1) = b_1, \qquad W_1(x, y_{N+1}) = b_2.$$

Evaluating the inner products (33b, c), using numerical integration to evaluate those inner products which involve the empirical functions L, G and $\mathrm{d}G/\mathrm{d}y$, results in a non-linear system of ordinary differential equations which may be written in the form

$$\mathbf{M}(\mathbf{W})\dot{\mathbf{W}} + h^{-1}\mathbf{S}(\mathbf{W})\mathbf{W} = h^{-1}\mathbf{F}(\mathbf{W}). \tag{34}$$

Discretizing this system of equations using the one-step θ method, in which the differentiated terms are approximated by

$$\dot{\mathbf{W}} \simeq (\mathbf{W}^{n+1} - \mathbf{W}^n)/k, \qquad k = x^{n+1} - x^n, \qquad n = 0, 1, 2, \ldots,$$

and the non-differentiated x-dependent terms by

$$\mathbf{W} \simeq \theta \mathbf{W}^{n+1} + (1-\theta)\mathbf{W}^n \equiv \mathbf{W}^{n+\theta},$$

results in the following system of non-linear algebraic equations which are to be solved for the unknown quantities $\mathbf{W}^{n+1}$:

$$[\mathbf{M}(\mathbf{W}^{n+\theta}) + \theta r\mathbf{S}(\mathbf{W}^{n+\theta})]\mathbf{W}^{n+1} = [\mathbf{M}(\mathbf{W}^{n+\theta}) - (1-\theta)r\mathbf{S}(\mathbf{W}^{n+\theta})]\mathbf{W}^n + r\mathbf{F}(\mathbf{W}^{n+\theta}), \tag{35}$$

where $r = k/h$ and $0 \leqslant \theta \leqslant 1$. The boundary conditions have been incorporated into (35) in the form

$$W_{1,1}^{n+1} = U_1^{n+1} = b_1(x^{n+1}), \qquad W_{1,N+1}^{n+1} = U_{N+1}^{n+1} = b_2(x^{n+1}).$$

The schemes defined by values of $\theta = 0, \frac{1}{2}, 1$ are the Euler, Crank–Nicolson and backward Euler Petrov–Galerkin schemes respectively, denoted by EPG, CNPG and BEPG.

By inspection of (35) it can be seen that for $\theta = 0$ the system is linear in $\mathbf{W}^{n+1}$ and for $\theta > 0$ it is non-linear. However, as shall be shown later, the EPG scheme, or strictly any scheme for which $\theta < \frac{1}{2}$, is not an appropriate scheme for solving (29). Therefore we shall henceforth assume $\frac{1}{2} \leqslant \theta \leqslant 1$. Among the many techniques available for solving non-linear systems such as (35) are the predictor–corrector (PC) method of Douglas and Dupont[35] and the well-known Newton–Raphson (NR) type methods. When considering (35), the former method has an advantage over NR in that it does not require specification of the Jacobian of the system. In this paper we shall describe only the PC technique; see Stewart[36] for details of the NR implementation. The PC technique requires (35) to be split into the following two linear subsystems:

$$\text{P:} \quad [\mathbf{M}(\mathbf{W}^n) + \theta r\mathbf{S}(\mathbf{W}^n)]\mathbf{W}_{(1)}^{n+1} = [\mathbf{M}(\mathbf{W}^n) - (1-\theta)r\mathbf{S}(\mathbf{W}^n)]\mathbf{W}^n + r\mathbf{F}(\mathbf{W}^n), \tag{36a}$$

$$\text{C:} \quad [\mathbf{M}(\mathbf{W}_{(i)}^{n+\theta}) + \theta r\mathbf{S}(\mathbf{W}_{(i)}^{n+\theta})]\mathbf{W}_{(i+1)}^{n+1} = [\mathbf{M}(\mathbf{W}_{(i)}^{n+\theta}) - (1-\theta)r\mathbf{S}(\mathbf{W}_{(i)}^{n+\theta})]\mathbf{W}^n + r\mathbf{F}(\mathbf{W}_{(i)}^{n+\theta}), \tag{36b}$$

where $i = 1, 2, 3, \ldots, I$ or until succeeding iterates have converged to within a specified tolerance, and

$$\mathbf{W}_{(i)}^{n+\theta} = \theta \mathbf{W}_{(i)}^{n+1} + (1-\theta)\mathbf{W}^n.$$

In practice it was found that one application of the corrector was usually sufficient to give reasonable results.

The structure of the linear systems (36) is of the form

$$\mathbf{A}\mathbf{W} = \mathbf{b}$$

where $\mathbf{A}$ is a $2(N+1) \times 2(N+1)$ block tridiagonal matrix and $\mathbf{W}$ and $\mathbf{b}$ are $2(N+1)$-vectors. Various efficient methods exist for the solution of such banded systems. Examples are the banded matrix algorithm in the LINPACK package[37] and the Keller block elimination algorithm.[38] The Keller algorithm proved to be very effective; details of the implementation can be found in Stewart.[36]

Boundary conditions

We require to impose two boundary conditions: one near the wall, external to the viscous sublayer; and the other at the outer edge of the turbulent boundary layer. We examine the specification of the latter condition first.

The outer edge boundary condition is

$$W_{1,N+1}^{n+1} = U_{N+1}^{n+1} = U_e(x^{n+1}), \qquad (N+1)h = \delta_+ > \delta^{n+1}, \tag{37}$$

where the boundary layer thickness $\delta^{n+1} = \delta(x^{n+1})$. To allow for the growth (or otherwise) of the turbulent boundary layer, we specify condition (37) by increasing (or decreasing) the number of nodes across the layer according to the increase (or decrease) in the boundary layer thickness. To estimate the change in δ, we appeal to the theory of characteristics outlined previously, in which it was noted that the outermost characteristic nominally coincides with the boundary layer edge. The angle between this characteristic curve and the x axis is given by

$$\eta_1 = \tan^{-1}\left(\frac{v+p+q}{u}\right).$$

Therefore, assuming that the characteristic curve is approximately linear, we have

$$\delta_+^{n+1} \simeq \delta_+^n + \Delta x^{n+1}\left(\frac{V+p+q}{U}\right)\Bigg|_{N+1}^{n}.$$

If the x step length Δx is set equal to the CFL step length, we can assume that the boundary layer thickness will not increase by more than one y step length, h, per x step length. Therefore a suitable procedure for defining the position of the outermost node is to add one additional node before solving the PC equations, setting $U_{N+2}^n = U_e(x^n)$, $T_{N+2}^n =$ tolerance and $U_{N+2}^{n+1} = U_e(x^{n+1})$. If, after solving the PC equations, it is found that $U_{N+1}^{n+1} > 0{\cdot}999\, U_e(x^{n+1})$ and $T_{N+1}^{n+1} <$ tolerance, then delete the added node $N+2$; otherwise set $N+1 \rightarrow N+2$ (see Figure 3).

Obviously, as the width of the boundary layer increases, the number of nodes, and hence the number of equations in the system (35), will increase, leading to the method employing a much smaller h step than is required for the assumed accuracy of the solutions. To keep the calculation 'optimal' in some sense, we employ the technique of Bradshaw *et al.*[8] in which a limit is imposed on the number of cross-stream nodes. When this limit is attained, the y step length is increased by the appropriate factor, with the number of nodes reset to the initial number. The values of U and T at the new nodes are found by interpolation.

An alternative to the above procedure is to use transformation techniques in which the region $[x_0, X] \otimes [\xi, \delta_+]$ is transformed into the rectangular region $[r_0, R] \otimes [0, 1]$. Such transformation techniques have been used in many variable/adaptive mesh algorithms. Details of such methods as applied to equations (29) can be found in Stewart.[36]

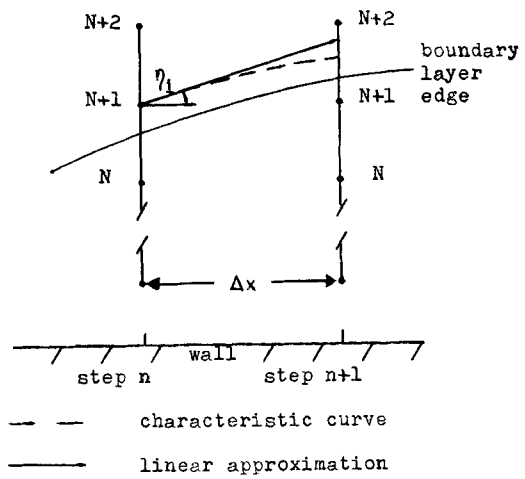

Figure 3. Geometry of the boundary conditions at the outer edge

We now consider the imposition of the near-wall boundary condition for the PC solution method. Near the wall the boundary condition to be imposed takes the form

$$W_{1,1}^{n+1} = U_1^{n+1} = u_\tau^{n+1}\left(\frac{1}{\kappa}\ln y_1^+ + C\right), \tag{38}$$

where y_1 must lie in the logarithmic law region, i.e., $y_1 > 30\text{–}50\nu/u_\tau^{n+1}$ and $u_\tau^{n+1} = \tau_w^{1/2}(x^{n+1})$. Note that (38) depends on the unknown skin friction coefficient $\tau_w^{1/2}(x^{n+1})$. Expressions of the general form

$$\tau_w = T_1 + y_1\left(\frac{\mathrm{d}}{\mathrm{d}x}(u_e^2) - \alpha\right)\Big/ 2 \tag{39}$$

have been derived by various authors to relate τ_w to known or calculable quantities. For example, Bradshaw *et al.*[39] define α to be

$$\alpha = 0{\cdot}3\frac{\mathrm{d}}{\mathrm{d}x}(U_1)^2, \tag{40a}$$

while Cebeci *et al.*[40] use

$$\alpha = \alpha^*\frac{\mathrm{d}\tau_w}{\mathrm{d}x}, \tag{40b}$$

where

$$\alpha^* = C_1(\ln y_1^+)^2 + C_2\ln y_1^+ + C_3 + C_4/y_1^+$$

and the constants C_i have values

$$C_1 = 5{\cdot}94884, \qquad C_2 = 13{\cdot}4882, \qquad C_3 = 13{\cdot}5718, \qquad C_4 = -698{\cdot}304.$$

An iterative procedure based on equations (38) and (39), where α is defined by either (40a) or (40b), which could be used to find τ_w^{n+1} consists of using the values available at step n to predict τ_w^{n+1} and hence U_1^{n+1}, updating these values after each solution of the predictor or corrector system. However, this method proved to be numerically unstable. To achieve a numerically stable procedure, it is necessary to impose an additional boundary condition, for T_1, at the near-wall boundary. To find the three unknowns U_1, T_1 and τ_w, the following procedure[39] is used prior to solving the PC system.

We have two equations (38) and (39) relating the three unknowns. An additional equation can be obtained from the ordinary differential equation along the wall pointing characteristic curve. Assuming that the characteristic curve is approximately linear, and employing central difference approximations, this equation can be written as

$$\begin{aligned} &T_B(U_1^{n+1} - U_A) - \frac{1}{2a_1}(p-q)\Big|_B (T_1^{n+1} - T_A) \\ &\quad = \left\{k\left(\frac{T}{U}\right)\left[u_e\frac{\mathrm{d}u_e}{\mathrm{d}x} + (p-q)\left(\frac{\mathrm{d}G}{\mathrm{d}y}T_m^{1/2} + \frac{T^{1/2}}{L}\right)\right]\right\}\Big|_B, \end{aligned} \tag{41}$$

where the points A and B lie along the line projected back from the first node point at the $(n+1)$st level and inclined at an angle

$$\eta_2 = \tan^{-1}\left(\frac{V+p-q}{U}\right)\Big|_1^{n+1}$$

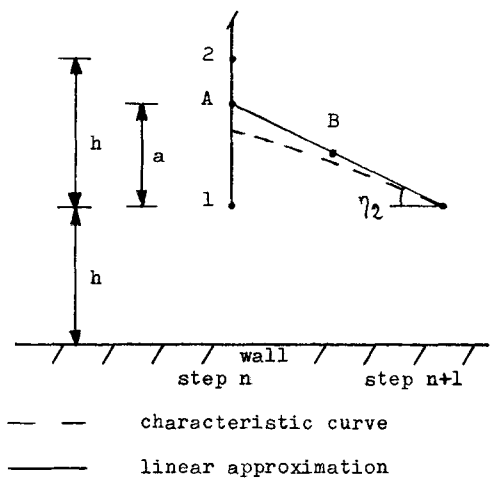

Figure 4. Geometry of the boundary conditions near the wall

to the x axis. A is the point where this linear approximation to the characteristic curve crosses $x = x^n$ and B is taken to be the midpoint of this line. Figure 4 illustrates the geometry.

If we set the x step length equal to the CFL step length, then we are assured that the point A lies between the first and second nodes. Assuming u and τ behave like logarithmic and linear functions respectively, the values of U_A and T_A are found by the interpolation process

$$U_A = rU_2 + (1-r)U_1, \qquad r = \ln(1+s)/\ln(2),$$
$$T_A = sT_2 + (1-s)T_1,$$

where $s = a/h = (k/h)\tan\eta_2$. The values at B are calculated as above using $s = (k/2h)\tan\eta_2$.

The near-wall boundary procedure therefore consists of solving equations (38), (39) and (41) simultaneously using Newton's method to give the required values at step $n+1$. The values of U_1 and T_1 are then used as boundary conditions for the solution of the PC equations.

Finding the transverse velocity v

Throughout the preceding it has been assumed that values for V_i, $i = 1, \ldots, N+1$, were known. A near-wall boundary condition for v can be derived,[8] namely

$$V_1^{n+1} = -U_1^{n+1} h \frac{\mathrm{d}}{\mathrm{d}x}\left(\ln u_\tau^{n+1}\right). \tag{42}$$

To find the internal values, we could apply the Petrov–Galerkin method with θ method time stepping to the continuity equation. This would give an $(N+1)\times(N+1)$ tridiagonal system which would be solved for V each time new values for U became available within the PC or NR iteration. However, by again appealing to the theory of characteristics, we can construct an alternative, elegant and less computationally expensive method. Recall that application of the existance condition (19) required that the ordinary differential equation (20) be satisfied by u, v and τ at every point $x \in [x_0, X]$. Discretizing (20) in space using the explicit Euler scheme and using (42) as an initial condition, we have an efficient and inexpensive procedure for calculating V_i, $i = 1, \ldots, N+1$.

Analysis of difference equations

The analysis given below is based on the simple scalar hyperbolic equation

$$u_t + cu_x = 0, \qquad t > 0, \qquad -\infty \leqslant x \leqslant \infty, \tag{43}$$

where c is assumed to be locally constant and greater than zero. Although (43) is a linear IVP, the results derived can supply valuable insight to the behaviour of the non-linear IBVP, equation (29).

Application of the PG method with θ method time stepping to equation (43) gives

$$\begin{aligned}&[(2+3\gamma)(U_{j-1}^{n+1} - U_{j-1}^{n}) + 8(U_j^{n+1} - U_j^n) + (2-3\gamma)(U_{j+1}^{n+1} - U_{j+1}^n)]\\ &\quad = -6r[-(1+\gamma)U_{j-1}^{n+\theta} + 2\gamma U_j^{n+\theta} + (1-\gamma)U_{j+1}^{n+\theta}],\end{aligned} \tag{44}$$

where $r = c\,\Delta t/h$.

The von Neumann analysis of fully discrete systems assumes solutions of the form

$$U_j^n = V^n e^{i\omega x_j}, \qquad |\omega h| < \pi, \tag{45}$$

where $x_j = jh$ (see, for example, Reference 41). Substitution of (45) into the difference equation (44) gives the characteristic equation for the amplification factor $z(\omega) = V^{n+1}/V^n$. The von Neumann stability criterion[41] states that the full discretization is stable if the solutions of the characteristic equation satisfy $|z(\omega)| \leqslant 1$ for all $|\omega| < \pi/h$.

For (44) the characteristic equation is

$$z(\omega) = \frac{1 + (1-\theta)A(\omega)}{1 - \theta A(\omega)},$$

where

$$A(\omega) = -6r\frac{2\gamma \sin^2(\omega h/2) + i\sin(\omega h)}{4 + 2\cos(\omega h) - i3\gamma \sin(\omega h)}.$$

By writing $z(\omega)$ in the form

$$z(\omega) = |z(\omega)|e^{i\arg z(\omega)} = |z(\omega)|e^{-i\omega c^* \Delta t},$$

where

$$c^*(\omega) = \frac{-\arg z(\omega)}{\omega\,\Delta t},$$

we can further investigate the properties of the fully discrete system by comparing the amplification factor with the ratio of the exact solution,

$$\frac{u(x, t+\Delta t)}{u(x,t)} = e^{-i\omega c \Delta t}.$$

Following Mitchell and Griffiths[17] and Richtmyer & Morton,[42] we say that a method is dissipative of order $2s$, with s a positive integer, if

$$|z(\omega)| \leqslant 1 - \sigma(\omega h)^{2s}$$

for σ a positive constant, $|\omega h| < \pi$. Further, the method is dispersive if $c^*(\omega) \neq c$.

Using Taylor series expansions we can derive the following expressions:

$$\begin{aligned}|z(\omega)| &= 1 - \tfrac{1}{2}(2\theta - 1)r^2(\omega h)^2 + \tfrac{1}{24}[(24\theta^3 - 24\theta^2 + 12\theta - 3)r^4 - \gamma r](\omega h)^4 + O(\omega h)^6,\\ \arg z &= -r(\omega h) + \tfrac{1}{3}(3\theta^2 - 3\theta + 1)r^3(\omega h)^3 + O(\omega h)^5,\end{aligned}$$

$$z - e^{-i\omega c\Delta t} = -\tfrac{1}{2}(2\theta - 1)r^2(\omega h)^2 + \tfrac{1}{6}i(6\theta^2 - 1)r^3(\omega h)^3 + \tfrac{1}{24}[(24\theta^3 - 1)r^4 - \gamma r](\omega h)^4 + O(\omega h)^5.$$

From the above we can deduce that:

(1) Any method for which $\theta < \frac{1}{2}$ is unstable in the sense of von Neumann for any value of γ. Conversely, if $\theta \geqslant \frac{1}{2}$, any γ, the method is stable.
(2) The method is conservative, i.e., non-dissipative, only when $\theta = \frac{1}{2}$ and $\gamma = 0$, i.e., the CNG method. For $\theta = \frac{1}{2}$, $\gamma \neq 0$, CNPG, the method is dissipative of order four. $\theta > \frac{1}{2}$ gives a dissipative method of order two, i.e., a diffusive method, irrespective of the value of γ.
(3) The method is dispersive of order two.
(4) The method is in general first-order accurate, with second-order accuracy only achieved when $\theta = \frac{1}{2}$.

5. NUMERICAL RESULTS AND DISCUSSION

In this section we present the numerical results from four test problems selected from the comprehensive series of numerical results available in Stewart.[36] The data for three of the four test problems are taken from the extensive set of test data compiled by Coles and Hirst.[43] The data for the other test problem can be found in the paper by Tsuji and Morikawa.[44] A brief description of the characteristics of all four test problems is given in Table I. Reading from left to right the entries in the Description column give the pressure gradient encountered as the flow moves downstream from the initial x station.

Results obtained using the CNG algorithm, i.e., the free parameters γ^1 and γ^2 are such that $\gamma^1 = 0 = \gamma^2$, are given in Figures 5(a) and 5(b). Figure 5(a) compares the U, T profiles calculated by the CNG algorithm with those calculated by the method of characteristics (MOC) algorithm of Bradshaw *et al.*[8,39] at selected points along the x axis for each test flow.

Figure 5(b) compares the integral flow parameters c_f, H and R_θ produced by CNG with those produced by the MOC algorithm and by experimental measurement. In addition, each test case has a diagram which plots the variable denoted DEL θ. This variable is a computational relative error estimate defined as follows:

$$\text{DEL}\,\theta := |\theta_1 - \theta_2|/\theta_2,$$

Table I. Description of numerical experiments

Originator and Reference	Description
Ludweig and Tillmann Ref. 43, ID = 1300	Moderately favourable
Wieghardt Ref. 43, ID = 1400	Zero
Schubauer and Klebanoff Ref. 43, ID = 2100	Favourable, ~ zero, strongly adverse, separation
Tsuji and Morikawa Ref. 44	Zero, adverse, favourable adverse, favourable

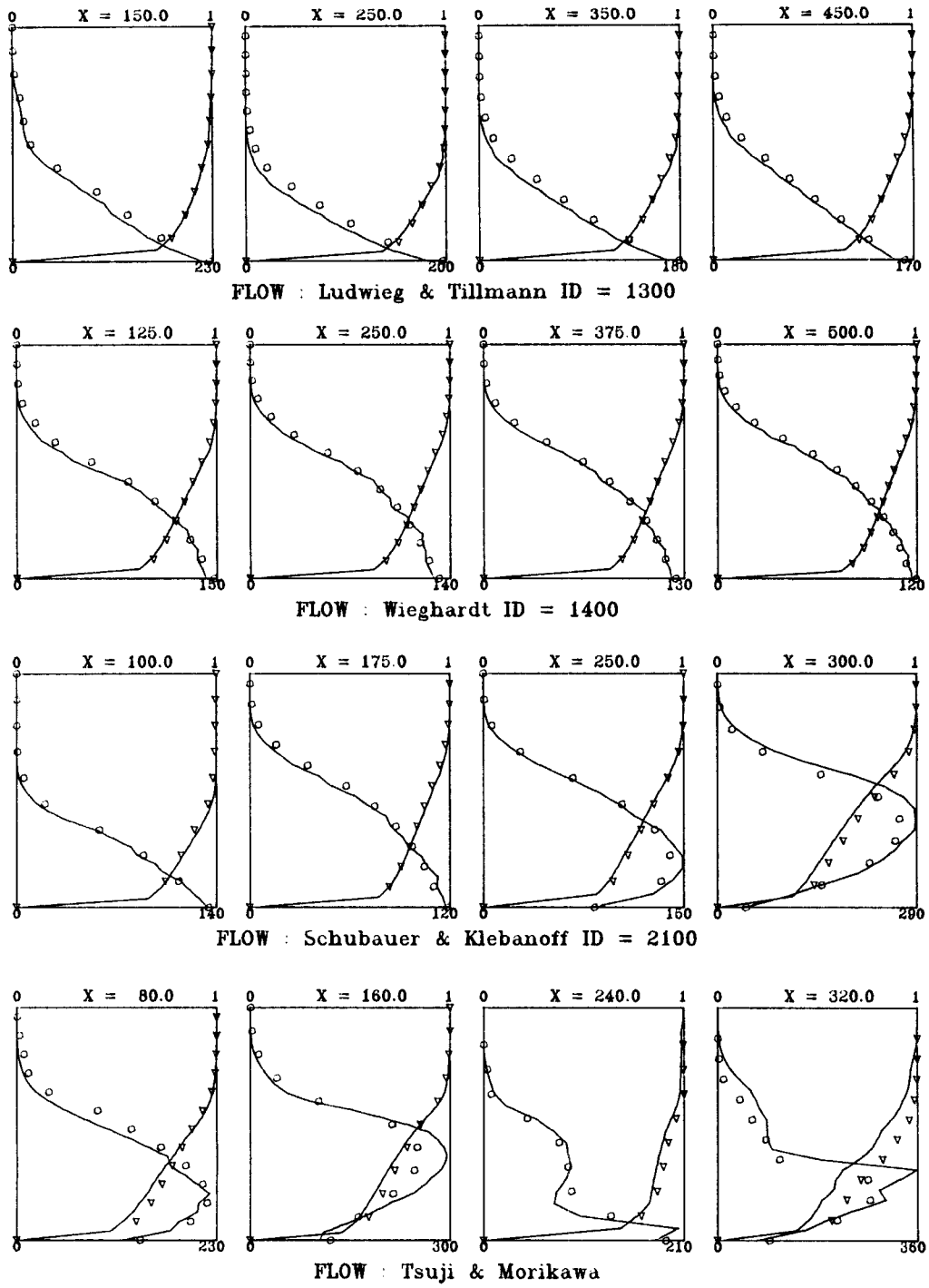

Figure 5(a). Comparison of the CNG method with MOC. U velocity and Reynolds shear stress profiles. The x stations and U/U_e ranges are shown at the top of each diagram. The range of $T \times 10^5$ is given at the foot of each diagram. Key: ○, Reynolds shear stress for MOC; V, U velocity profile for MOC; ——, U velocity profile and Reynolds shear stress profiles for finite element methods

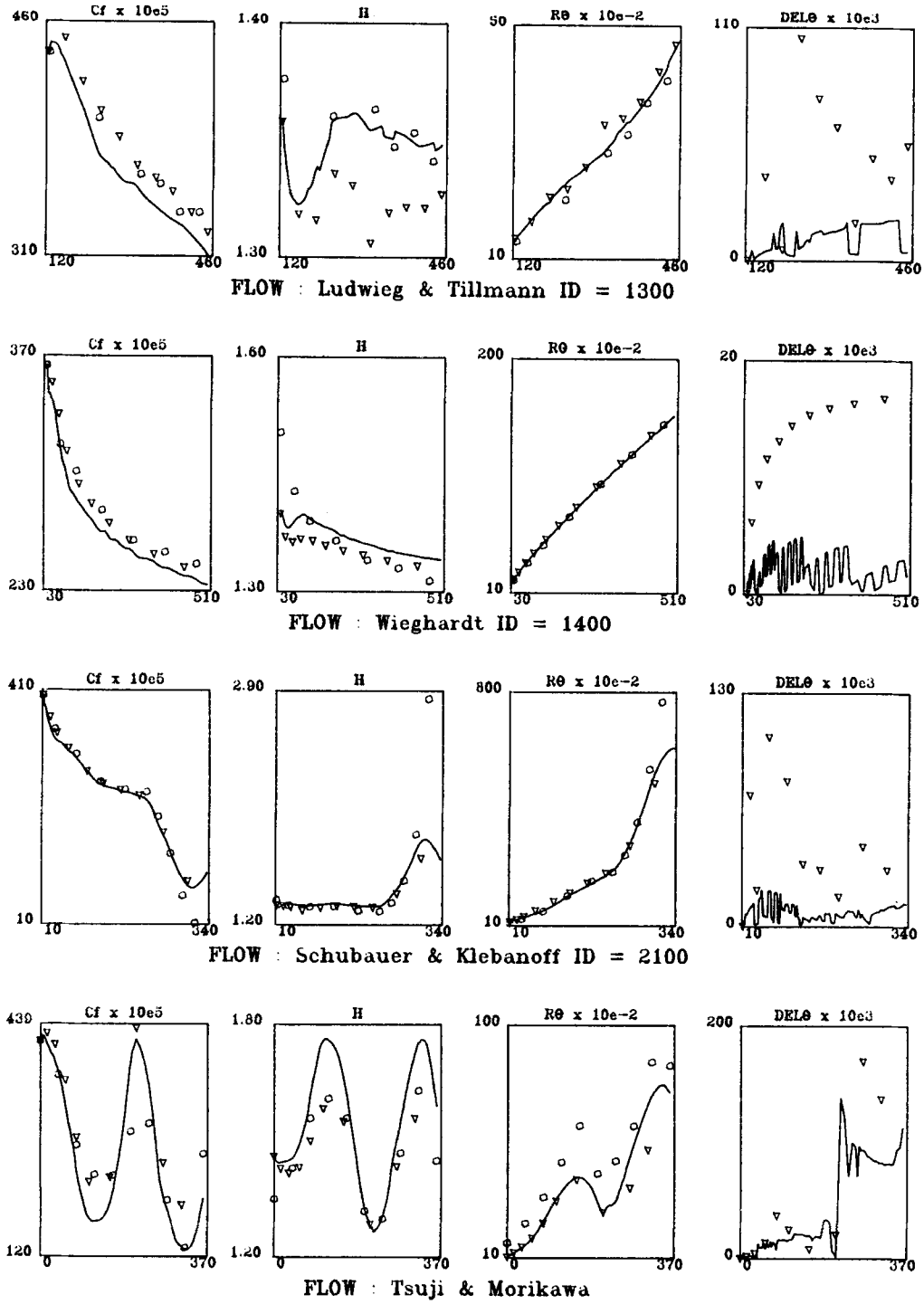

Figure 5(b). Comparison of the CNG method with MOC. Graphs of the integral flow parameters c_f, H, R_θ and DEL θ. The range of x stations is given at the foot of each diagram. The function ranges are given at the left-hand side of each diagram. Key: ○, experimental readings; ∇, results from MOC; ——, results from finite element methods

where θ_1 is the value of θ calculated from the momentum thickness definition,[30] i.e.,

$$\theta := \int_0^{\delta+} \left(1 - \frac{u}{u_e}\right)\frac{u}{u_e}\,dy, \tag{46}$$

and θ_2 is the value of θ calculated from the momentum integral equation,[30] i.e.,

$$\frac{d}{dx}(u_e^2\theta) + \delta^* u_e \frac{du_e}{dx} = \tau_w. \tag{47}$$

Note that as (46) and (47) are defined under the same assumptions employed in constructing the TSL equations, the computational relative error estimate is only valid in regions where the TSL assumptions hold; for example, the estimate should not be considered accurate or valid within regions where the flow is close to separation.

As is evident from Figure 5(a), the CNG solutions, although acceptable in terms of accuracy in comparison with the MOC solutions, exhibit oscillations; mainly in the Reynolds shear stress profiles. For flows without large gradients in the solution profiles these wiggles may be acceptable. However, for flows in which large gradients appear in the solution profiles the oscillations can adversely affect the solution to a significant degree. For example, in the latter stages of the Tsuji and Morikawa test case it can be seen that the CNG method does not accurately model the U, T profiles in the vicinity of the 'knee point'.[44] However, a comparison of the DEL θ parameters for CNG and MOC (Figure 5(b)) shows that the CNG method gives a significant improvement in computational accuracy.

The oscillations in the solution profiles produced by CNG prompted the development of the CNPG algorithm, in which the free parameters γ^1 and γ^2 are now generally non-zero. Recall that while the CNG method is conservative (non-dissipative), the CNPG method is fourth-order dissipative. The most appropriate values for γ^1 and γ^2 were found by numerical experimentation to be the following:

Momentum equation

$$\gamma_j^1 = \lambda_j^1 \frac{\Delta x}{h} = \left(\frac{V_j + (p+q)|_j}{U_j}\right)\frac{\Delta x}{h}, \qquad j = 1, \ldots, N, \tag{48}$$

Shear stress equations

$$\gamma_j^2 = \lambda_j^2 \frac{\Delta x}{h} = \left(\frac{V_j + (p-q)|_j}{U_j}\right)\frac{\Delta x}{h}, \qquad j = 1, \ldots, N, \tag{49}$$

where λ_1 and λ_2 are the eigenvalues of the system (29a) given by equations (22). Therefore the free parameters are different for each equation and vary both across (y direction) and along (x direction) the boundary layer. In other words they are flow-dependent.

Numerical results produced by CNPG with the parameters γ^1 and γ^2 defined by (48), (49) are given in Figures 6(a) and 6(b).

Comparing Figure 6(a) with Figure 5(a), it can be seen that the oscillations have been almost completely eliminated. There are a few oscillations present near the start for some flows, e.g., Wieghardt at $x = 125$. These oscillations are caused by inconsistencies between the experimental initial and boundary values and, as can be seen, are soon damped by the CNPG method. Comparing the U, T solution profiles given in Figures 5(a) and 6(a) and the DEL θ graphs given in Figures 5(b) and 6(b), it can be seen that the accuracy of the standard Galerkin method has not been compromised by the fourth-order dissipative CNPG method.

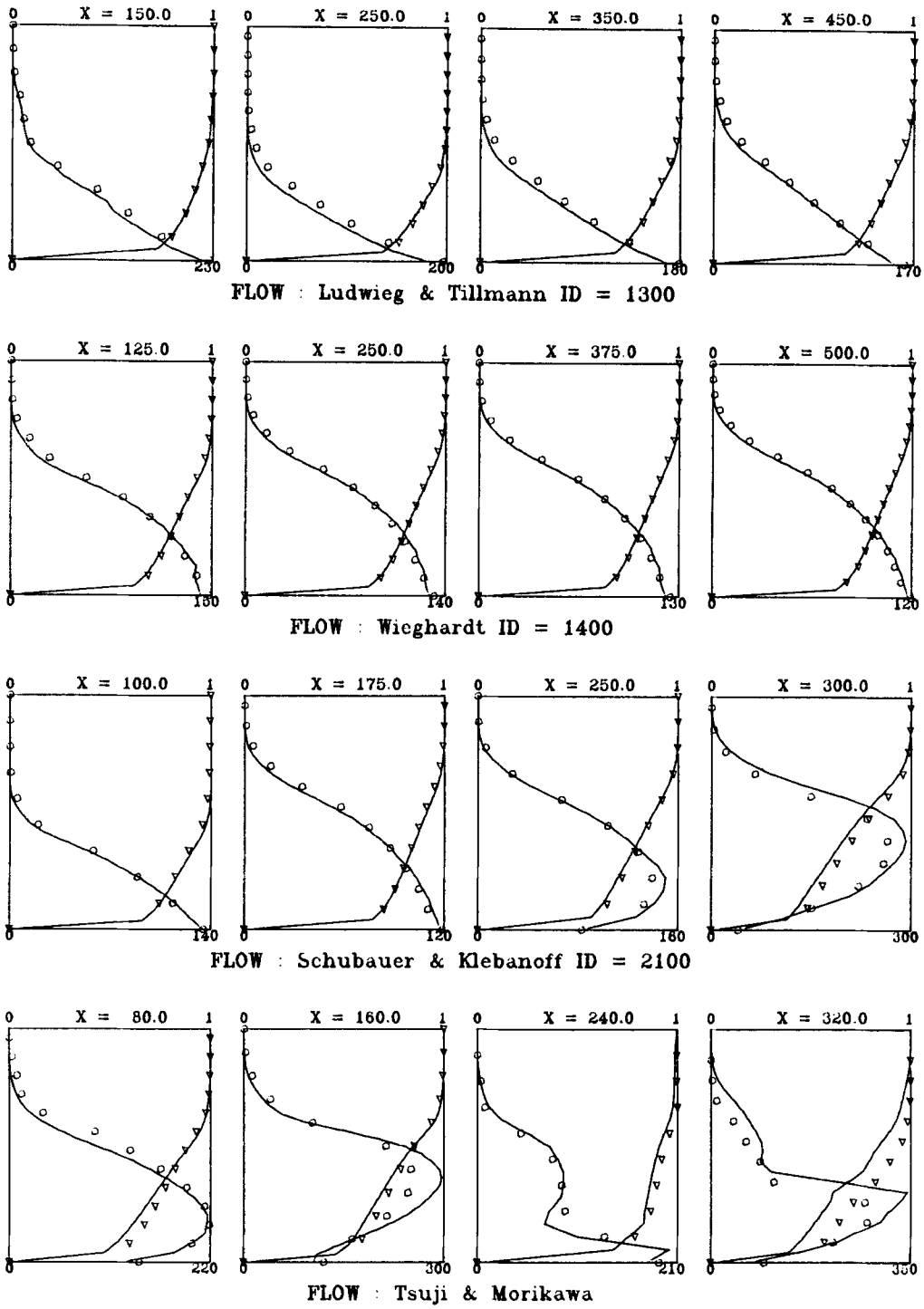

Figure 6(a). Comparison of the CNPG method with MOC. Diagram annotation as per Figure 5(a)

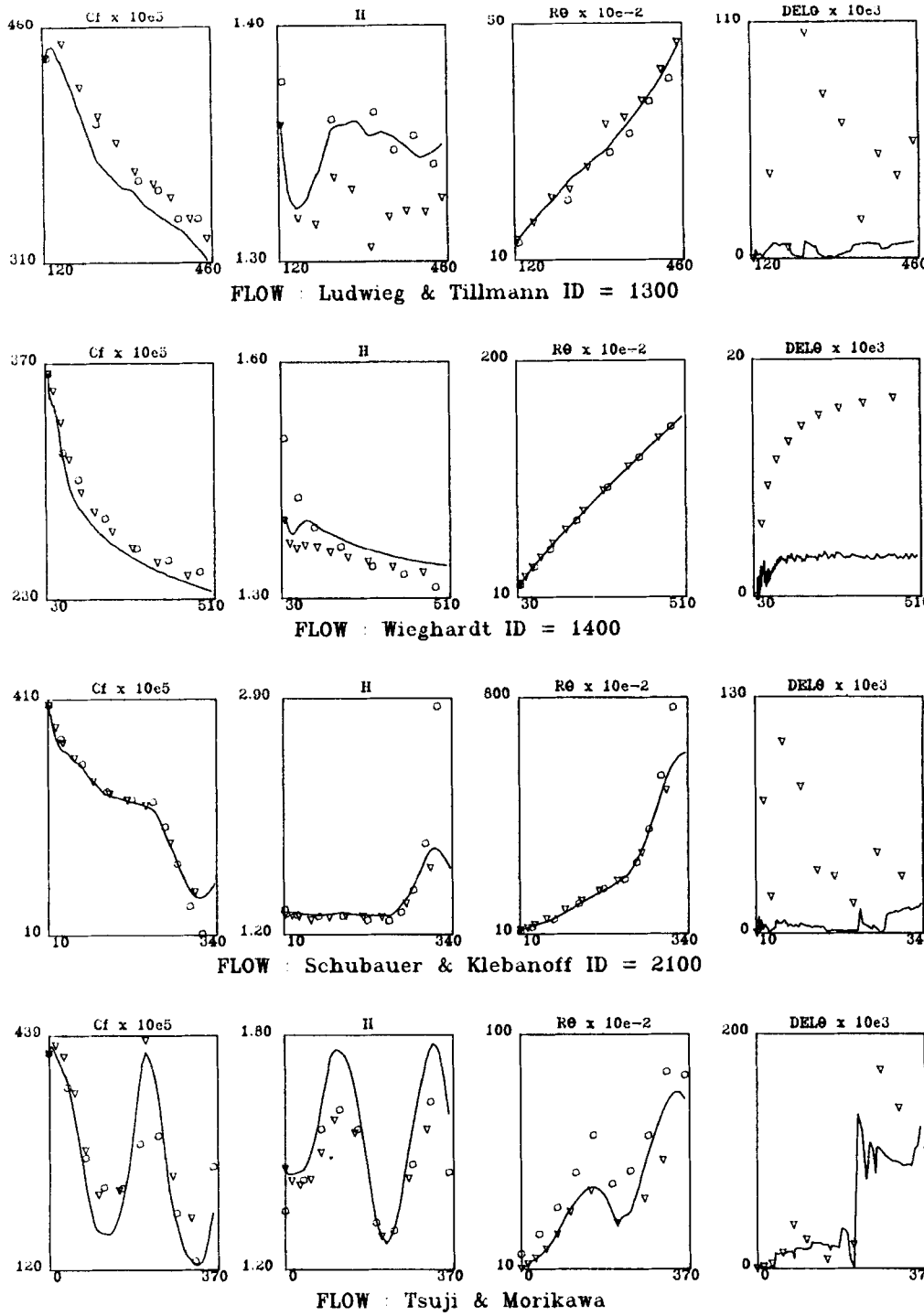

Figure 6(b). Comparison of the CNPG method with MOC. Diagram annotation as per Figure 5(b)

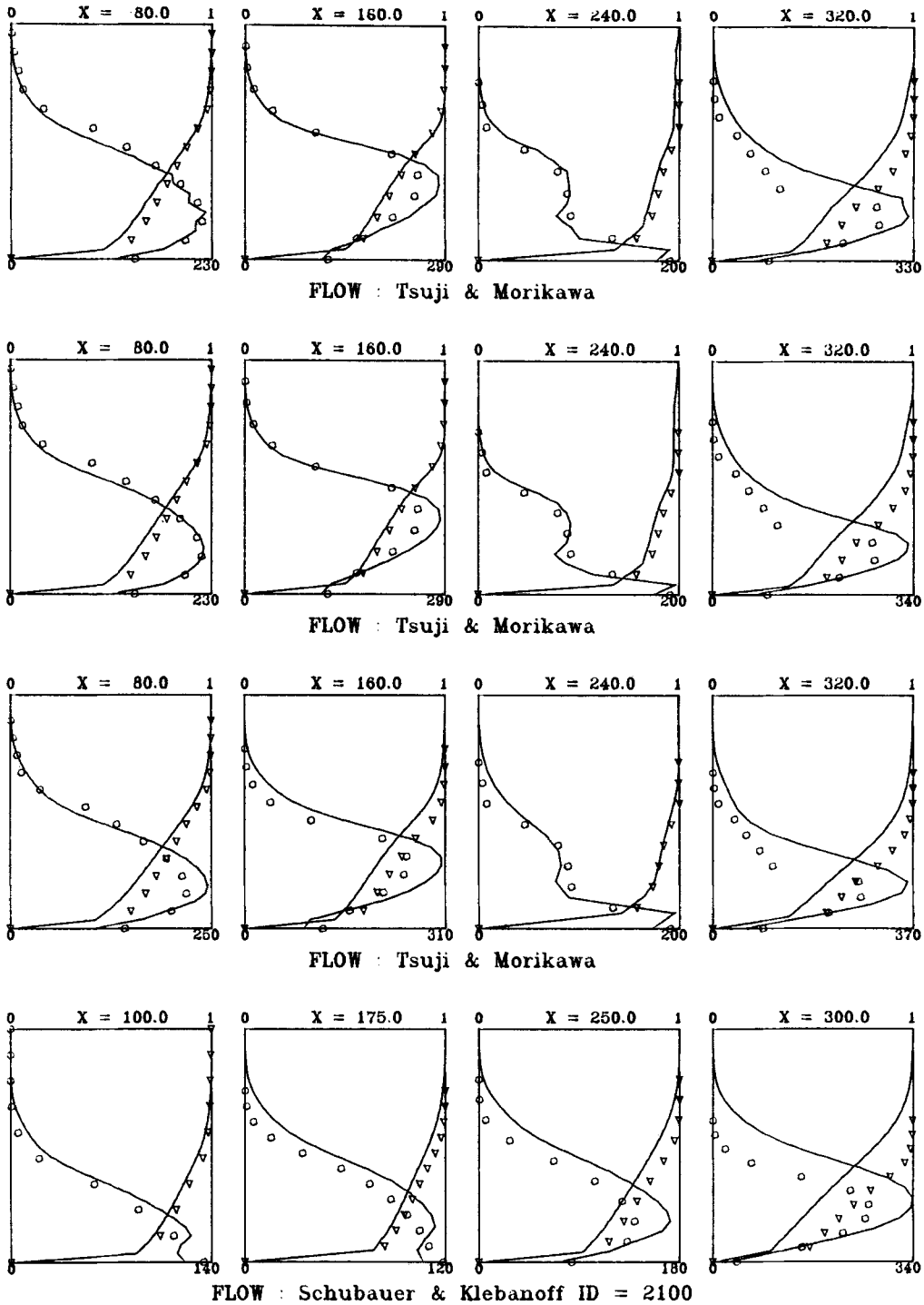

Figure 7(a). Comparison of the BEG, BEPG and PLEG methods with MOC. Diagram annotation as per Figure 5(a)

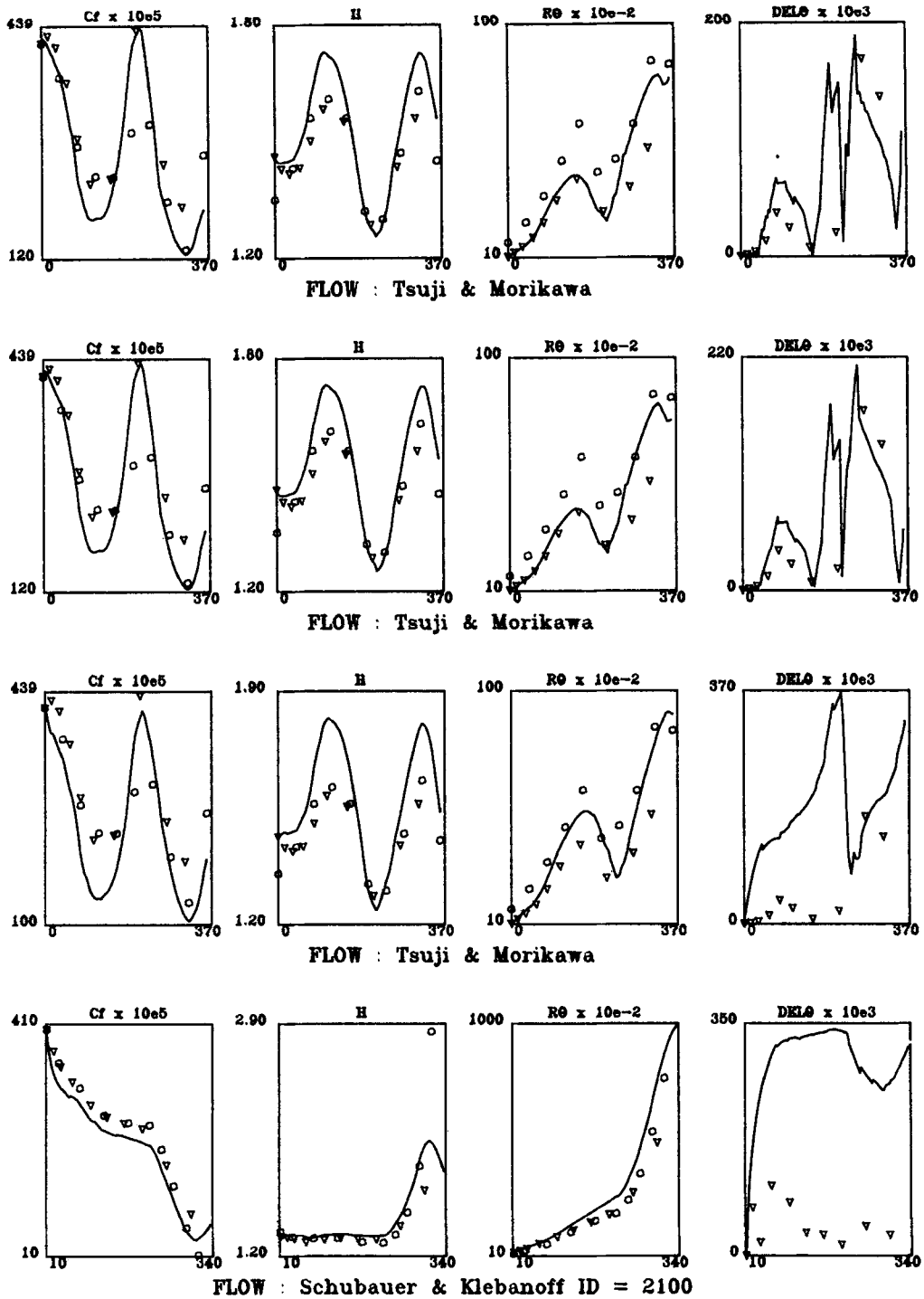

Figure 7(b). Comparison of the BEG, BEPG and PLEG methods with MOC. Diagram annotation as per Figure 5(b)

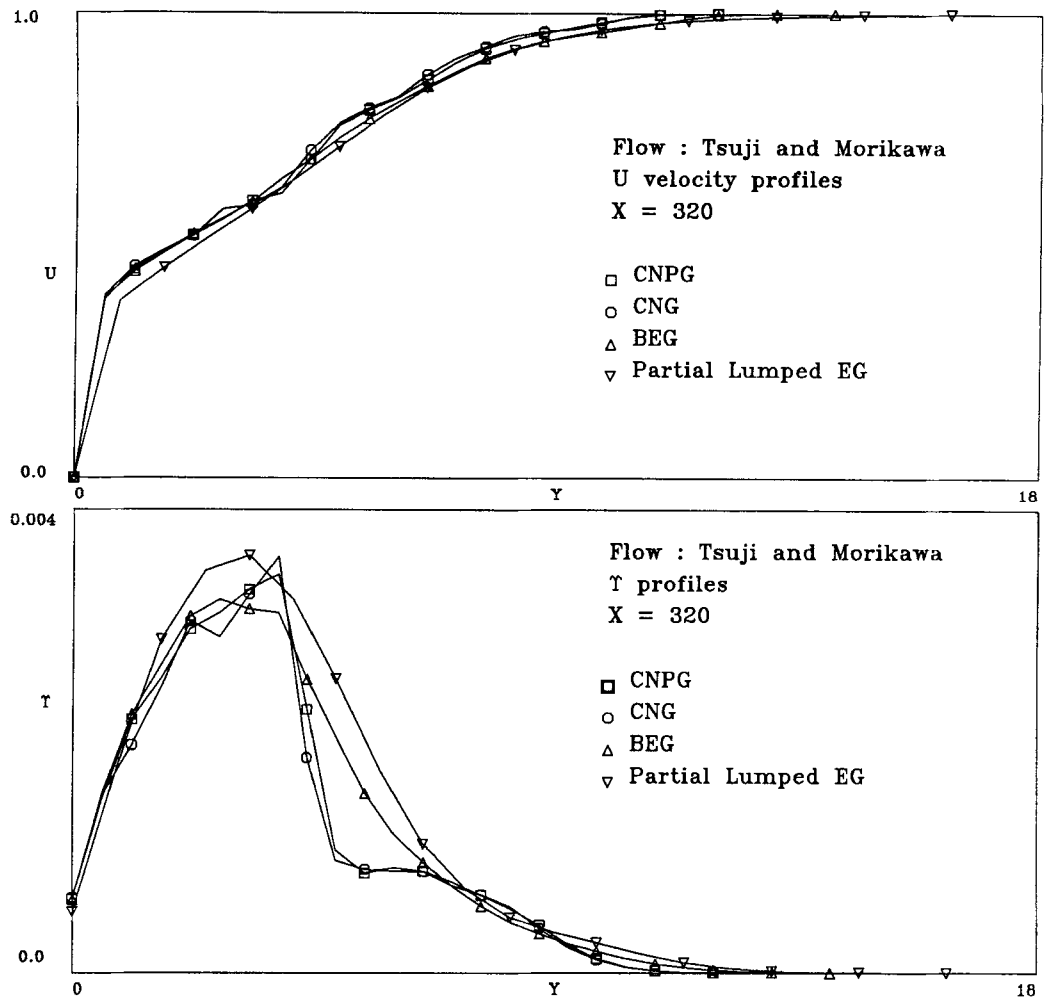

Figure 8. Comparison of the CNPG, CNG, BEG and PLEG methods for the Tsuji and Morikawa test problem

Other θ method techniques

Recall that setting $\theta = 0$ entails using the explicit Euler method as the time stepping scheme, giving the EG and EPG methods, while setting $\theta = 1$ entails using the backward Euler scheme, giving the BEG and BEPG methods.

It was shown in Section 4 that the EG and EPG schemes were unstable for the scalar hyperbolic equation. This is also the case for the non-linear hyperbolic system (29). The numerical instability of the EG scheme for hyperbolic equations has been known for some time, as has the fact that conditional stability can be achieved by partial lumping (see, for example, Reference 17). By contrast, using the techniques for analysing difference equations outlined in Section 5, it can be shown that the partially lumped EPG scheme is not consistent with the differential equation.

However, although the partially lumped EG scheme (PLEG) is stable, the solutions produced by the scheme are poor. Examples are given in the bottom two test flows of Figures 7(a) and 7(b), i.e., Tsuji and Morikawa, Schubauer and Klebanoff, and also in Figure 8. From Figure 7(b) it can be

seen that the accuracy of the method as measured by DEL θ is significantly worse than that of the MOC.

The top two test flows in Figures 7(a) and 7(b) are produced by the BEG and BEPG schemes respectively. In Section 4 it was shown that both BEG and BEPG schemes are second-order dissipative, i.e., diffusive, schemes. The effect of this inherent diffusivity in both methods is clearly seen in the U, T solution profiles at $x = 320$ for the Tsuji and Morikawa test flow, where the sharp change in the solutions at the knee point have been completely smoothed. See also Figure 8 for a more detailed comparison. Note also that the accuracy of the BEG and BEPG methods as measured by DEL θ is comparable with the MOC.

6. CONCLUSIONS

In this paper we have constructed a numerical scheme for solving the Bradshaw, Ferriss and Atwell turbulence model for 2D constant property turbulent boundary layers. The numerical results produced by the method for a selection of turbulent boundary layer test data have been presented.

The system of equations comprising the BFA turbulence model was shown to be ill-posed and a modified problem was stated. The equations of this modified problem were shown to be of hyperbolic type and the equations for the eigenvalues and characteristic curves were derived. The ordinary differential equations along the characteristic curves were also derived. The numerical scheme was constructed by employing the Petrov–Galerkin technique to discretize the equations in the y direction. The resulting non-linear ordinary differential equations are integrated in the x direction by the θ method. To specify the near-wall boundary condition in the numerical scheme, it was necessary for numerical stability to employ the ordinary differential equation along the wall pointing characteristic. The position of the outer edge of the turbulent boundary layer was calculated using a linear approximation to the relevant characteristic curve. The oscillations that occurred in the CNG solutions were eliminated by setting the free parameters γ^1 and γ^2 in the CNPG method to simple functions of the eigenvalues of the system.

We have demonstrated that the Petrov–Galerkin technique has potential in the numerical solution of hyperbolic systems of partial differential equations. However, we do not claim that the particular test functions employed, i.e., equations (32), are the only, or even the best, possible test functions. Other types of test function have been proposed by various authors, for example, Griffiths and Mitchell[34] and Morton and Parrott.[19]

REFERENCES

1. P. Bradshaw (ed.), *Turbulence (Topics in Applied Physics 12)*, Springer-Verlag, Berlin, 1976.
2. T. Cebeci and A. M. O. Smith, *Analysis of Turbulent Boundary Layers*, Academic Press, New York, 1974.
3. B. E. Launder and D. B. Spalding, *Mathematical Models of Turbulence*, Academic Press, London, 1972.
4. A. B. Haines, 'Turbulence modelling—report of a working party', *Aeronaut. J.*, **86**, 269–277 (1982).
5. W. Rodi, 'Examples of turbulence models for incompressible flows', *AIAA J.*, **20**, 872–879 (1982).
6. W. Rodì, *Turbulence Models and their Application in Hydraulics—a State of the Art Review*, IAHR Publication, Delft, 1980.
7. J. G. Marvin, 'Turbulence modelling for computational aerodynamics', *AIAA J.*, **21**, 941–955 (1983).
8. P. Bradshaw, D. H. Ferriss and N. P. Atwell, 'Calculation of boundary layer development using the turbulent energy equation', *J. Fluid Mech.*, **28**, 593–616 (1967).
9. P. J. Roache, *Computational Fluid Dynamics*, Hermosa Publishers, Albuquerque, New Mexico, 1972.
10. A. J. Baker, *Finite Element Computational Fluid Mechanics*, McGraw-Hill, New York, 1983.
11. J. J. Connor and C. A. Brebbia, *Finite Element Techniques for Fluid Flow*, Newnes-Butterworths, London, 1976.
12. A. G. Hutton, 'A survey of the theory and application of the finite element method in the analysis of viscous incompressible, Newtonian flow', *CEGB Report No. RD/B/N3049*, 1974.
13. G. Strang and G. J. Fix, *An Analysis of the Finite Element Method*, Prentice-Hall, Englewood Cliffs, New Jersey, 1973.

14. A. R. Mitchell and R. Wait, *The Finite Element Method in Partial Differential Equations*, Wiley, New York, 1977.
15. I. Christie and A. R. Mitchell, 'Upwinding of high order Galerkin methods in conduction–convection problems', *Int. j. numer. methods eng.*, **12**, 1746–1771 (1978).
16. I. Christie, D. F. Griffiths, A. R. Mitchell and O. C. Zienkiewicz, 'Finite element methods for second order differential equations with significant first derivatives', *Int. j. numer. methods eng.*, **10**, 1389–1396 (1976).
17. A. R. Mitchell and D. F. Griffiths, *The Finite Difference Method in Partial Differential Equations*, Wiley, New York, 1980.
18. A. R. Mitchell and D. F. Griffiths, 'Semi-discrete generalised Galerkin methods for time-dependent conduction–convection problems', *Dundee NA Report 24*, 1978.
19. K. W. Morton and A. K. Parrott, 'Generalised Galerkin methods for first order hyperbolic equations', *J. Comput. Phys.*, **36**, 249–270 (1980).
20. A. G. Hutton and R. M. Smith, 'On the finite element simulation of incompressible turbulent flow in general two-dimensional geometries', *CEGB Report No. 5010N81*, 1981.
21. B. E. Launder and D. B. Spalding, 'The numerical computation of turbulent flow', *Comput. Methods Appl. Mech. Eng.*, **3**, 269–289 (1974).
22. K. Morgan, T. G. Hughes and C. Taylor, 'Investigation of a mixing length and a two equation turbulence model utilizing the finite element method', *Appl. Math. Modelling*, **1**, 395–400 (1977).
23. K. Morgan, T. G. Hughes and C. Taylor, 'A numerical model of turbulent shear flow behind a prolate spheroid', *Appl. Math. Modelling*, **2**, 271–274 (1978).
24. M. O. Soliman and A. J. Baker, 'Accuracy and convergence of a finite element algorithm for turbulent boundary layer flow', *Comput. Methods Appl. Mech. Eng.*, **28**, 81–102 (1981).
25. R. M. Smith, 'On the finite element calculation of turbulent flow using the k–ε model', *Int. j. numer. methods fluids*, **4**, 303–319 (1984).
26. R. M. Smith, 'A practical method of two-equation turbulence modelling using finite elements', *Int. j. numer. methods fluids*, **4**, 321–336 (1984).
27. C. Taylor, T. G. Hughes and K. Morgan, 'A numerical analysis of turbulent flow in pipes', *Comput. Fluids*, **5**, 191–204 (1977).
28. A. A. Townsend, *The Structure of Turbulent Shear Flow (2nd edn)*, Cambridge University Press, Cambridge, 1976.
29. P. Bradshaw, 'The strategy of calculation methods for complex turbulent flow', *IC Aero Report 73–05*, 1973.
30. H. Schlichting, *Boundary Layer Theory*, McGraw-Hill, New York, 1968.
31. A. Jeffrey, *Quasilinear Hyperbolic Systems and Waves*, Pitman, London, 1976.
32. R. Courant and D. Hilbert, *Methods of Mathematical Physics Volume II*, Interscience, New York, 1962.
33. R. D. Richtmyer, *Principles of Advanced Mathematical Physics, Vol. I*, Springer-Verlag, Berlin, 1978.
34. D. F. Griffiths and A. R. Mitchell, 'On generating upwind finite element methods', in T. J. R. Hughes (ed.), *Finite Element Methods for Convection Dominated Flows (AMD Vol. 34)*, 1979.
35. J. Douglas and T. Dupont, 'Galerkin methods for parabolic equations', *SIAM J. Numer. Anal.*, **7**, 575–626 (1970).
36. I. B. Stewart, 'Investigation of the application of the finite element method to turbulent boundary layer calculations', *Ph.D. Thesis*, University of Dundee, 1985.
37. J. J. Dongarra, C. B. Moler, J. R. Bunch and G. W. Stewart, *LINPACK User's Guide*, SIAM, Philadelphia, 1979.
38. H. B. Keller, 'Accurate difference methods for two-point boundary value problems', *SIAM J. Numer. Anal.*, **11**, 305–320 (1974).
39. P. Bradshaw and K. Unsworth, 'An improved FORTRAN program for the Bradshaw–Ferriss–Atwell method of calculating turbulent shear layers', *IC Aero Report 74–02*, 1974.
40. T. Cebeci, K. C. Chang and P. Bradshaw, 'Solution of a hyperbolic system of turbulence model equations by the 'box' method', *Comput. Methods Appl. Mech. Eng.*, **22**, 213–227 (1980).
41. R. Vichnevetsky and J. B. Bowles, *Fourier Analysis of Numerical Approximations of Hyperbolic Equations (SIAM Studies in Applied Maths 5)*, SIAM, Philadelphia, 1982.
42. R. D. Richtmyer and K. W. Morton, *Difference Methods for Initial Value Problems*, Wiley, New York, 1967.
43. D. Coles and E. A. Hirst (eds), *Proc. Computation of Turbulent Boundary Layers—1968 AFOSR-IFR-Stanford Conf. Vol. 2*, Thermosciences Division, Stanford University, 1969.
44. Y. Tsuji and Y. Morikawa, 'Turbulent boundary layer with pressure gradient alternating in sign', *Aeronaut. Q.*, **27**, 15–28 (1976).